Effect of Hydrostatic Pressures of up to 9 GPa on the Galvanomagnetic Properties of Cd_3As_2–MnAs (20 mol % MnAs) Alloy in a Transverse Magnetic Field

L. A. Saypulaeva[a], M. M. Gadzhialiev[a], A. G. Alibekov[a], N. V. Melnikova[b], V. S. Zakhvalinskii[c], A. I. Ril'[d, *], S. F. Marenkin[d, e], T. N. Efendieva[a], I. V. Fedorchenko[d], and A. Yu. Mollaev[a]

[a] *Amirkhanov Institute of Physics, Dagestan Scientific Center, Russian Academy of Sciences, ul. Yaragskogo 94, Makhachkala, 367003 Dagestan, Russia*

[b] *Ural Federal University, ul. Mira 19, Yekaterinburg, 620002 Russia*

[c] *Belgorod State National Research University, ul. Pobedy 85, Belgorod, 308015 Russia*

[d] *Kurnakov Institute of General and Inorganic Chemistry, Russian Academy of Sciences, Leninskii pr. 31, Moscow, 119991 Russia*

[e] *Moscow Institute of Steel and Alloys (National University of Science and Technology), Leninskii pr. 4, Moscow, 119991 Russia*

Abstract—We have studied the effect of hydrostatic pressure on the galvanomagnetic properties of a Cd_3As_2 + 20 mol % MnAs alloy in a transverse magnetic field of up to 4 kOe. The pressure dependences of the Hall coefficient and resistivity for the alloy provide evidence of reversible phase transitions. The observed negative magnetoresistance of the alloy is shown to be induced by high pressure.

Keywords: high hydrostatic pressure, Hall effect, resistivity, negative magnetoresistance, structural phase transition

INTRODUCTION

Cd_3As_2–MnAs alloys have attracted considerable interest because they consist of Cd_3As_2, a narrow-band-gap semiconductor [1–3], and MnAs, a well-known ferromagnet [4]. The constituent components of this system are of interest for producing granulated spintronic structures [5]. Based on results of theoretical and experimental studies, Cd_3As_2 is thought to be a three-dimensional topological Dirac semimetal (3D TDS). Angle-resolved photoelectron spectroscopy [1] and scanning tunneling microscopy results demonstrate the existence of 3D Dirac fermions in this compound. 3D Dirac semimetals exhibit unusual effects: quantum spin Hall effect, giant diamagnetism, and others. Cadmium arsenide is more attractive for investigation of these effects than are well-known 3D TDS compounds, for example, Na_3Bi, because they are hygroscopic. Cd_3As_2 is a basic compound for studies of unique phases, such as Weyl semimetals, axion dielectrics, and topological superconductors. Not only Cd_3As_2 [6, 7] but also Cd_3As_2-based diluted magnetic semiconductors [8–10] are of interest as spintronic materials.

The diluted magnetic semiconductors have been studied as injectors of spin-polarized charge carriers. There is, however, a problem related to the fact that the coefficient of electron spin injection across a ferromagnetic metal–semiconductor interface is not very large because of the resistance mismatch between the layers. This problem can be resolved by utilizing diluted magnetic semiconductors, such as GaMnAs, and Mn–V (MnP, MnAs, and MnSb) magnetic semimetal compounds [10–13]. At temperatures below their Curie temperature (T_C), solid solutions of diluted magnetic semiconductors have an internal magnetic field, and exchange interaction between Mn ions usually increases with increasing Mn concentration owing to the decrease in Mn–Mn distance. Cd_3As_2–MnAs alloy containing 20 mol % MnAs consists of a $(Cd_{1-x}Mn_x)_3As_2$ solid solution with inclusions of another ferromagnetic phase, MnAs, with T_C = 318 K [14, 15]. Thus, the alloy comprises two interacting magnetic subsystems: solution of Mn ions in a highly conductive medium (Cd_3As_2 Dirac semimetal) and ferromagnetic MnAs, which allows us to envisage the possibility of creating an injection material with a high degree of polarization.

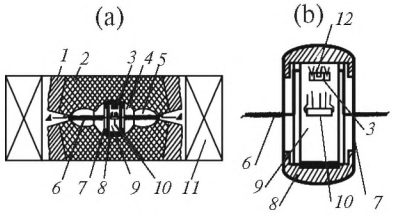

Fig. 1. Schematic of the apparatus used to generate hydrostatic pressures of up to 9 GPa: (*1*) steel matrices, (*2*) VK-6 hard alloy inset, (*3*) manganin pressure gage, (*4*) catlinite toroid, (*5*) catlinite gasket, (*6*) wire lead, (*7*) Teflon capsule, (*8*) copper lids, (*9*) pressure-transmitting medium, (*10*) sample, (*11*) solenoid, (*12*) bismuth reference sensor; (a) apparatus, (b) Teflon capsule.

There is currently great interest in more accurately determining the band structure of the Cd_3As_2 semiconductor. This issue has been addressed for a rather long time, and in a number of studies band inversion was assumed along with a zero-gap state [1, 16–18]. The evolution of bands in ternary and quaternary cadmium arsenide-based solid solutions is of interest as a separate issue, but at the same time it extends our understanding of the properties of Cd_3As_2 as a three-dimensional Dirac semimetal. The existence of 3D Dirac fermions allows one to explain the anomalously high carrier mobility in single crystals of this compound [3]. Note that the carrier concentration in it can be controlled by doping, in particular by adding manganese.

This paper presents a continuation of our detailed studies of the electrical, galvanomagnetic, and thermoelectric properties of alloys in the Cd_3As_2–MnAs system [15, 19, 20] in wide ranges of temperatures, pressures, and magnetic fields.

EXPERIMENTAL

Cd_3As_2–MnAs alloy containing 20 mol % MnAs is a composite consisting of MnAs ferromagnetic nanogranules and a Cd_3As_2 semiconductor matrix. The alloy was synthesized by reacting the Cd_3As_2 and MnAs compounds under vacuum in graphitized silica ampules at the melting point of manganese arsenide [20]. According to differential thermal analysis (DTA) and X-ray diffraction characterization results, the alloy had the form of a composite in which the α''-Cd_3As_2 phase prevailed.

High pressures were generated in a Toroid chamber, which generated high hydrostatic pressures of up to 9 GPa. Figure 1 shows a schematic of the chamber and a high-pressure cell.

The transport and galvanomagnetic properties (resistivity, Hall coefficient, and magnetoresistance) of the alloy were studied by a standard four-probe technique. A magnetic field was generated by a multiturn solenoid with a magnetic field strength $H \sim 5$ kOe. The samples had the form of rectangular parallelepipeds 3 × 1.0 × 1.0 mm in dimensions. The current passing through the samples was monitored with a Keithley 2000 digital multimeter. To characterize the system under investigation, we considered the magnetic field H, the current I through the sample, Hall voltage V_H, resistivity ρ, and pressure p. The measurements were performed at two opposite current and field directions.

The resistivity of the sample was calculated using the formula

$$\rho = \frac{V_H ab}{Il_p},$$

where V_H is the measured voltage, a is the width of the sample, b is the thickness of the sample, I is the current through the sample, and l_p is the separation between the probes.

In Hall effect measurements, we used a direct current I and static magnetic field H. A static magnetic field of 4 kOe was generated by a coil. To reduce the contribution of extraneous electromotive forces to the measured Hall voltage V_H, we averaged the results obtained by measuring the total transverse voltage at two current directions (I^- and I^+) and two field directions (B^- and B^+):

$$V_H = \frac{+V_{I^+B^+} - V_{I^-B^+} + V_{I^-B^-} - V_{I^+B^-}}{4},$$

$$R_H = \frac{V_H d}{IH},$$

where d is the thickness of the sample. To a good approximation, R_H can be thought of as a constant characteristic of the material. R_H is determined by electron and hole concentrations and mobilities in the material. If current carriers are only free electrons, we have $R_H = 1/(ne)$, where n is the electron concentration and e is the electron charge. Magnetoresistance (MR) was determined as $\frac{MR - MR_0}{MR_0} \times 100\%$.

RESULTS AND DISCUSSION

Characterization of the samples. Figure 2 presents X-ray powder diffraction results for the Cd_3As_2 + 20 mol % MnAs alloy. Its X-ray diffraction pattern shows reflections from both the α''-Cd_3As_2 phase and MnAs phase.

The DTA and X-ray diffraction results are supported by scanning electron microscopic (SEM) examination of the surface of the alloy. Figure 3 shows SEM images of the surface of the 80 mol % Cd_3As_2 + 20 mol % MnAs alloy. Most of the sample is uniform in composition, which corresponds to the Cd_3As_2 compound according to elemental analysis data.

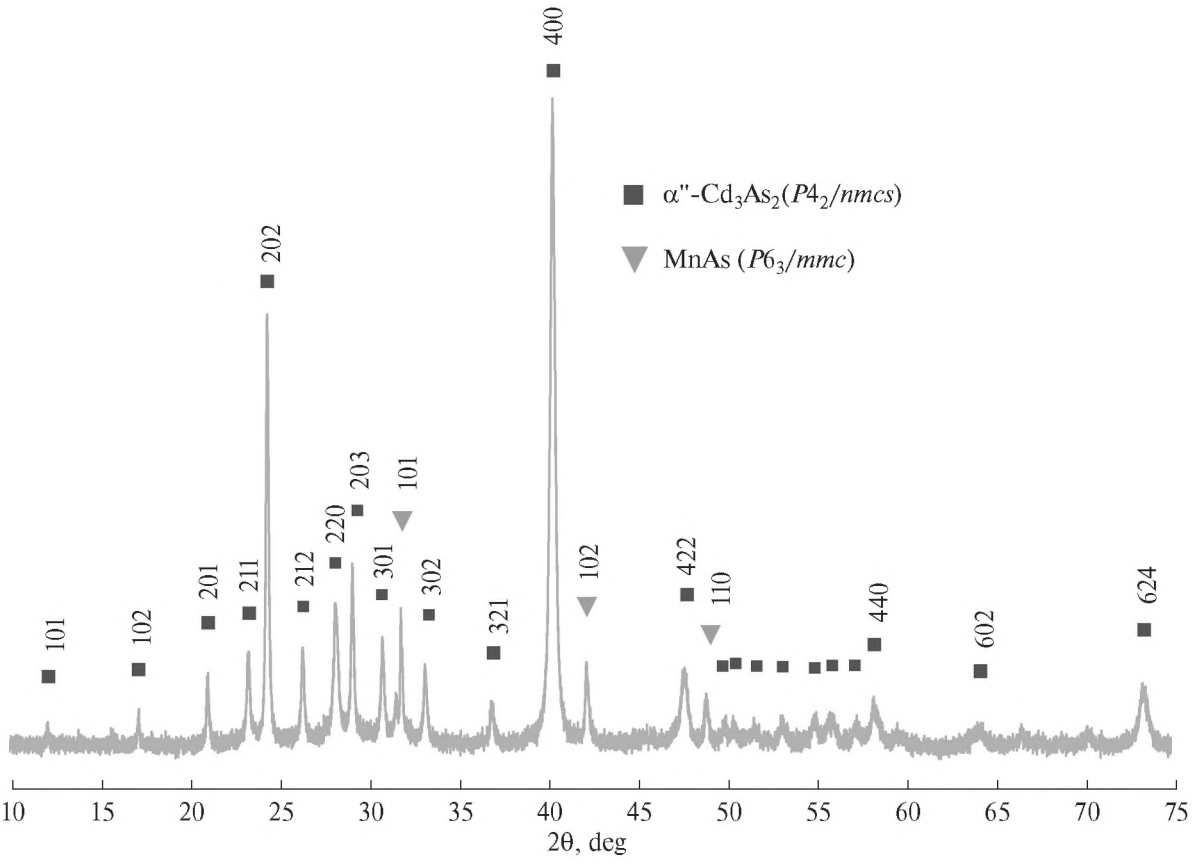

Fig. 2. X-ray diffraction pattern of the 80 mol % Cd_3As_2 + 20 mol % MnAs sample.

Additional inclusions account for less than 5% of the sample area. They are arsenic-enriched and cadmium-deficient compared to the matrix. A magnified image of the alloy microstructure (Fig. 3, inset) demonstrates that there is a complex distribution of the constituent elements and that the sample contains submicron inclusions similar in composition to Cd_3As_2. Elemental analysis of a dark area corresponding to an inclusion indicates that the second phase is $CdAs_2$.

Electrical resistance. Electrical properties depend on the size and packing density of granules. If the average density of particles is low, the material has rather low electrical conductivity. At a high density, when a considerable number of particles are in contact with each other, the structure may contain rather extended clusters, and the conductivity of such structure will not obey the additivity rule. The real conductivity of the alloy will be determined by the conductivity of the MnAs and Cd_3As_2 phases, the interfacial layer between them, and the shape of the granules. The carrier tunneling probability is determined by the size of the granules; the distance between them; the tunneling barrier height, width, and shape; and temperature.

Figure 4 shows the temperature dependence of resistivity, $\rho(T)$, for the Cd_3As_2 + 20 mol % MnAs alloy in the temperature range 77–450 K. Characteristically, the alloy has metallic conductivity.

Figure 5 shows resistivity as a function of increasing and decreasing pressure. As the pressure is raised to 2.8 GPa, the resistivity of the alloy rises very gradually

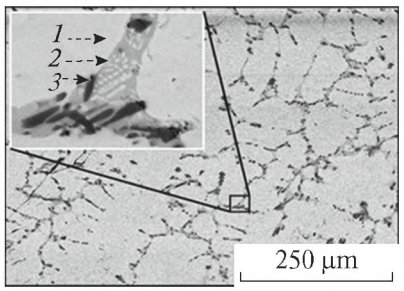

Point	Cd	As	Mn
1	56.9	38.8	4.3
2	37.7	62.3	–
3	3.6	48.4	48.0

Fig. 3. SEM image of the surface of the alloy and quantitative elemental analysis data at the points indicated by arrows in the inset.

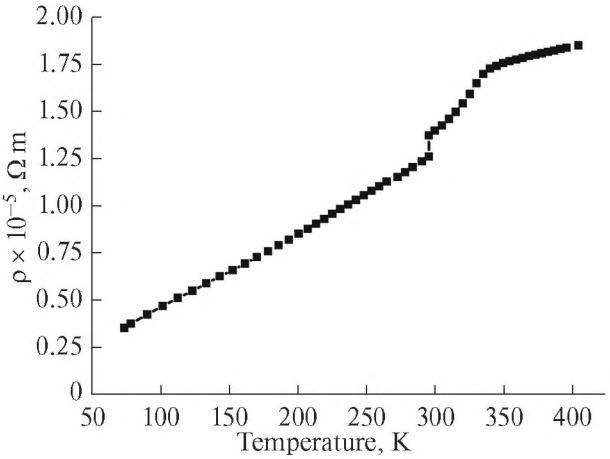

Fig. 4. Temperature dependence of resistivity.

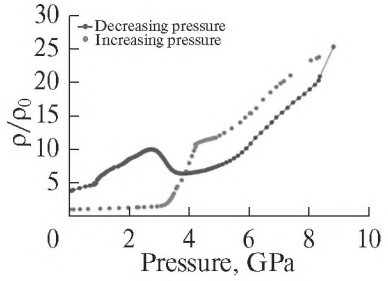

Fig. 5. Reduced resistivity as a function of increasing and decreasing pressure.

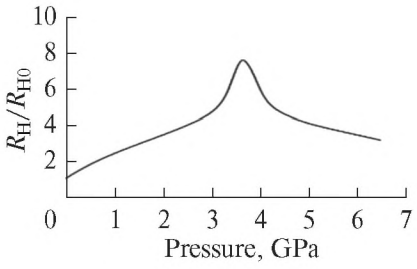

Fig. 6. Reduced Hall coefficient as a function of pressure for the Cd_3As_2 + 20 mol % MnAs alloy (R_H and R_{H0} are the Hall coefficients of the material in a magnetic field and in zero field, respectively).

and monotonically. At higher pressures, it rises sharply, reaching a maximum at 4.2 GPa. As the pressure is released, the resistivity drops at a varying rate and has a maximum at 2.75 GPa.

Hall coefficient. Figure 6 shows the Hall coefficient as a function of pressure, $R_H(p)$. At ≈3.65 GPa, the Hall coefficient passes through a maximum. Its behavior correlates with the ρ(p) pressure dependence, which also has a sharp peak at ≈4.2 GPa. The reversible peaks in the ρ(p) and $R_H(p)$ pressure dependences point to a structural transformation of the alloy.

Magnetoresistance. Figure 7 shows magnetoresistance as a function of magnetic field at constant pressure. Magnetoresistance as a function of pressure at constant magnetic field is shown in Fig. 8. The data demonstrates a negative magnetoresistance, with a maximum (~1%) in the pressure range ≈1–2.6 GPa. In addition to the negative magnetoresistance, the behavior of the positive magnetoresistance of the alloy has specific features in the pressure range corresponding to the phase transitions of the Cd_3As_2 semiconductor matrix of the composite and the MnAs ferromagnetic granules [19, 21].

The pressure dependences of the resistivity, Hall coefficient, and magnetoresistance have characteristic features due to a phase transition in the pressure range 3–4 GPa. The peak in the pressure dependence of reduced magnetoresistance rises with increasing magnetic field strength. The behavior of electrical characteristics of composites with a different MnAs concentration was also reported to have distinctive features in the vicinity of 4 GPa [14, 19, 21].

Thus, it is reasonable to assume that, under the effect of high pressures, the Cd_3As_2 + 20 mol % MnAs alloy undergoes a joint phase transition in the Cd_3As_2 matrix and MnAs ferromagnet. In the range 2.6–4.0 GPa, Cd_3As_2 undergoes a transition from a tetragonal to a monoclinic structure, which supports previously reported data [22, 23]. At pressures in the range 3.5–3.8 GPs, MnAs undergoes spin reorientation transitions, which influence the electrical properties and magnetoresistance of the composite.

The mechanism behind the development of a negative magnetoresistance in granulated structures was addressed in a number of studies [24–26]. In the absence of a magnetic field, the angle between the magnetic moments of ferromagnetic clusters is random. An applied magnetic field aligns the magnetic moments in the field direction, leading to a marked drop in resistivity. Magnetoresistance is proportional to the magnetic field, the cosine of the angle between the magnetic moments, and the number of ferromagnetic clusters.

High pressures reduce the distance between the MnAs granules. The transport properties of composites are determined by not only charge transport processes within the granules but also carrier tunneling between the granules. If the granule size is comparable to the size of magnetic domains, an applied magnetic field aligns the magnetic moments of the granules in the field direction, reducing conduction electron scattering and leading to a negative magnetoresistance. Tunneling resistance decreases with increasing external magnetic field, as it causes ordering of the magnetization of individual domains. With increasing pres-

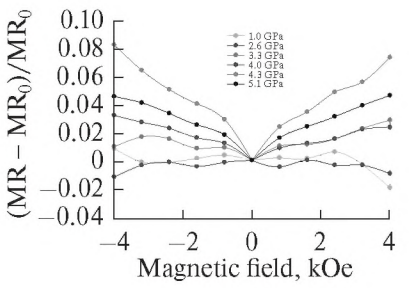

Fig. 7. Magnetoresistance as a function of magnetic field at constant pressure for the Cd_3As_2 + 20 mol % MnAs alloy.

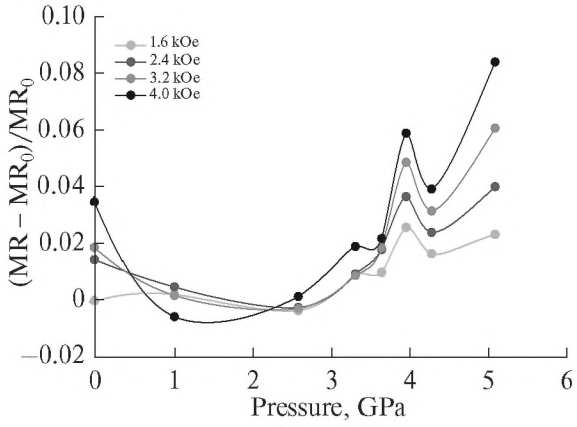

Fig. 8. Magnetoresistance as a function of pressure at constant magnetic field for the Cd_3As_2 + 20 mol % MnAs alloy.

sure, the tunneling resistance decreases owing to the reduction in the distance between the granules, that is, owing to the reduction in tunneling barrier height. Moreover, it should be taken into account that the matrix of the composite contains electrically active defects produced during the synthesis of the composite material and the formation of the MnAs granules. Some of the defects are uncompensated atoms with a nonzero spin, which act as localized magnetic moments or magnetic centers of carrier scattering in a magnetic field.

CONCLUSIONS

The present results demonstrate that, at high pressures, the Cd_3As_2 + 20 mol % MnAs alloy has a negative magnetoresistance due to changes in tunneling conditions because of the reduction in the distance between the magnetic moments of the ferromagnet and to the structural transition of the semiconductor matrix.

Under high hydrostatic pressures, the magnetoresistance of Cd_3As_2–MnAs alloys exhibits complex behavior.

REFERENCES

1. Liu, Z.K., Jiang, J., Zhou, B., Wang, Z.J., Zhang, Y., Weng, H.M., Prabhakaran, D., Mo, S.-K., Peng, H., Dudin, P., Kim, T., Hoesch, M., Fang, Z., Dai, X., Shen, Z.X., Feng, D.L., Hussain, Z., and Chen, Y.L., A stable three-dimensional topological Dirac semimetal Cd_3As_2, *Nat. Mater.,* 2014, no. 7, pp. 677–681. https://doi.org/10.1038/NMAT3990
2. Lazarev, V.B., *Poluprovodnikovye soedineniya gruppy $A^{II}B^{V}$* (II–V Compound semiconductors), Moscow: Nauka, 1978.
3. Marenkin, S.F. and Trukhan, V.M., *Fosfidy, arsenidy tsinka i kadmiya* (Zinc and Cadmium Phosphides and Arsenides), Minsk: Varaskin A.N., 2010.
4. Okamoto, H., The As–Mn (arsenic–manganese) system, *Bull. Alloy Phase Diagrams,* 1989, vol. 10, no. 5, pp. 549–554. https://doi.org/10.1007/BF02882414
5. Shchelkachev, N.M. and Yarzhemsky, V.G., Influence of crystal structure and 3d impurities on the electronic structure of the topological material Cd_3As_2, *Inorg. Mater.,* 2018, vol. 54, no. 11, pp. 1093–1098. https://doi.org/10.1134/S0020168518110110
6. Wang, Z., Weng, H., Wu, Q., Dai, X., and Fang, Z., Three-dimensional Dirac semimetal and quantum transport in Cd_3As_2, *Phys. Rev. B: Condens. Matter Mater. Phys.,* 2013, vol. 88, no. 12, paper 125 427. https://doi.org/10.1103/PhysRevB.88.125427
7. Borisenko, S., Gibson, Q., Evtushinsky, D., Zabolotnyy, V., Buchner, B., and Cava, R.J., Experimental realization of a three-dimensional Dirac semimetal, *Phys. Rev. Lett.,* 2014, vol. 113, no. 2, paper 027 603. https://doi.org/10.1103/PhysRevLett.113.027603
8. Arushanov, E.K., II_3V_2 compounds and alloys, *Prog. Crystal Growth Character.,* 1992, vol. 25, no. 3, pp. 131–201. https://doi.org/10.1016/0960-8974(92)90030-T
9. Lu, H., Zhang, X., and Jia, S., Topological phase transition in single crystals of $(Cd_{1-x}Zn_x)_3As_2$, *Sci. Rep.,* 2017, vol. 7, paper 3148. https://doi.org/10.1038/s41598-017-03559-2
10. Prokof'eva, M.M., Dorokhin, M.V., Danilov, Yu.A., Kudrin, A.V., and Vikhrova, O.V., Electroluminescence of InGaAs/GaAs heterostructures with (III,Mn)V and Ni ferromagnetic injectors, *Semiconductors,* 2010, vol. 44, no. 11, pp. 1398–1401. https://doi.org/10.1134/S1063782610110035
11. Marenkin, S.F., Kochura, A.V., Izotov, A.D., and Vasil'ev, M.G., Manganese pnictides MnP, MnAs, and MnSb are ferromagnetic semimetals: preparation, structure, and properties (a survey), *Russ. J. Inorg. Chem.,* 2018, vol. 63, no. 14, pp. 1753–1763. https://doi.org/10.1134/S0036023618140036
12. Jungwirth, T., Sinova, J., Malek, J., Kuchera, J., and MacDonald, A.H., Theory of ferromagnetic (III,Mn)V semiconductors, *Rev. Mod. Phys.,* 2006, vol. 78, no. 3, pp. 809–863. https://doi.org/10.1103/RevModPhys.78.809
13. Ploog, K.H., Epitaxial ferromagnet–semiconductor heterostructures for electrical spin injection, *J. Cryst. Growth,* 2004, vol. 268, nos. 3–4, pp. 329–335. https://doi.org/10.1016/j.jcrysgro.2004.04.050

14. Melnikova, N.V., Tebenkov, A.V., Sukhanova, G.V., Babushkin, A.N., Saipulaeva, L.A., Zakhvalinskii, V.S., Gabibov, S.F., Alibekov, A.G., and Mollaev, A.Y., Thermoelectric properties of a ferromagnetic semiconductor based on a Dirac semimetal (Cd_3As_2) under high pressure, *Phys. Solid State,* 2018, vol. 60, no. 3, pp. 494–498. https://doi.org/10.1134/S1063783418030174
15. Govor, G.A., First-order phase transition in manganese arsenide, *Phys. Solid State,* 2015, vol. 57, no. 5, pp. 871–872. https://doi.org/10.1134/S1063783415050121
16. Cisowski, J., Semimagnetic semiconductors based on II–V compounds, *Phys. Status Solidi B*, 1997, vol. 200, no. 2, pp. 311–350.
17. Ivanov, O., Zakhvalinskii, V., Nikulicheva, T., Yaprintsev, M., and Ivanichikhin, S., Asymmetry and parity violation in magnetoresistance of magnetic diluted Dirac–Weyl semimetal $(Cd_{0.6}Zn_{0.36}Mn_{0.04})_3As_2$, *Phys. Status Solidi Rapid Res. Lett.,* 2018, vol. 12, no. 12, paper 1800386. https://doi.org/10.1002/pssr.201800386
18. Aubin, M.J., Caron, L.G., and Jay-Gerin, J.-P., Band structure of cadmium arsenide at room temperature, *Phys. Rev. B: Condens. Matter Mater. Phys.,* 1977, vol. 15, no. 8, pp. 3872–3878. https://doi.org/10.1103/PhysRevB.15.3872
19. Alibekov, A.G., Mollaev, A.Y., Saipullaeva, L.A., Marenkin, S.F., Fedorchenko, I.V., and Ril', A.I., Hall effect, electrical and magnetic resistance in Cd_3As_2 + MnAs (30%) composite at high pressures, *Russ. J. Inorg. Chem.,* 2017, vol. 62, no. 1, pp. 90–93. https://doi.org/10.1134/S003602361701003X
20. Ril, A.I., Fedorchenko, I.V., Marenkin, S.F., Kochura, A.V., and Kuz'ko, A.E., Phase equilibria in the $CdAs_2$–Cd_3As_2–MnAs ternary system, *Russ. J. Inorg. Chem.,* 2017, vol. 62, no. 7, pp. 976–986. https://doi.org/10.1134/S0036023617070191
21. Alibekov, A.G., Mollaev, A.Yu., Saipullaeva, L.A., Marenkin, S.F., and Fedorchenko, I.V., Magnetotransport effects in granular Cd_3As_2 + MnAs structures at high pressures, *Inorg. Mater.,* 2016, vol. 52, no. 4, pp. 357–360. https://doi.org/10.1134/S0020168516040014
22. He, L., Jia, Y., Zhang, S., Hong, X., Jin, C., and Li, S., Pressure-induced superconductivity in the three-dimensional topological Dirac semimetal Cd_3As_2, *Quantum Mater.,* 2016, no. 1, paper 16 014. https://doi.org/10.1038/npjquantmats.2016.14
23. Glazkov, V.P., Kozlenko, D.P., Podurets, K.M., Savenko, B.N., and Somenkov, V.A., Neutron diffraction investigation of the atomic and magnetic structures of MnAs at high pressures, *Crystallogr. Rep.,* 2003, vol. 48, no. 1, pp. 54–57.
24. Ershov, A.A. and Krutova, J.A., Asymptotics of magnetoresistance, *Vestn. Yuzhno-Ural. Gos. Univ., Ser. Vych. Mat. Inf.,* 2016, vol. 5, no. 1, pp. 5–12. https://doi.org/10.14529/cmse160101
25. Marenkin, S.F., Izotov, A.D., Fedorchenko, I.V., and Novotortsev, V.M., Manufacture of magnetic granular structures in semiconductor–ferromagnet systems, *Russ. J. Inorg. Chem.,* 2015, vol. 60, no. 3, pp. 295–300. https://doi.org/10.1134/S0036023615030146
26. Marenkin, S.F., Trukhan, V.M., Fedorchenko, I.V., Trukhanov, S.V., and Shelkovaya, T.V., Magnetic and electrical properties of Cd_3As_2 + MnAs composite, *Russ. J. Inorg. Chem.*, 2014, vol. 59, no. 4, pp. 355–359. https://doi.org/10.1134/S0036023614040111